2022 21st ACM/IEEE International Conference on Information Processing in Sensor Networks (IPSN) | 978-1-6654-9624-7/22/$31.00 ©2022 IEEE | DOI: 10.1109/IPSN54338.2022.00033

An Energy Supervisor Architecture for Energy-Harvesting Applications

Nurani Saoda
University of Virginia
saoda@virginia.edu

Wenpeng Wang
University of Virginia
wangwp@virginia.edu

Md Fazlay Rabbi Masum Billah
University of Virginia
masum@virginia.edu

Bradford Campbell
University of Virginia
bradjc@virginia.edu

ABSTRACT

Energy-harvesting designs typically include highly entangled application-level and energy-management subsystems that span both hardware and software. This tight integration makes developing sophisticated energy-harvesting systems challenging, as developers have to consider both embedded system development and intermittent energy management simultaneously. Even when successful, solutions are often monolithic, produce suboptimal performance, and require substantial effort to translate to a new design. Instead, we propose a new energy-harvesting power management architecture, Altair that offloads all energy-management operations to the power supply itself while making the power supply programmable.

Altair introduces an energy supervisor and a standard interface to enable an abstraction layer between the power supply hardware and the running application, making both replaceable and reconfigurable. To ensure minimal resource conflict on the application processor, while running resource-hungry optimization techniques in the supervisor, we implement the Altair design in a lower power microcontroller that runs in parallel with the application. We also develop a programmable power supply module and a software library for seamless application development with Altair.

We evaluate the versatility of the proposed architecture across a spectrum of IoT devices and demonstrate the generality of the platform. We also design and implement an online energy-management technique using reinforcement learning on top of the platform and compare the performance against fixed duty-cycle baselines. Results indicate that sensors running the online energy-manager perform similar to continuously powered sensors, have a 10× higher event generation rate than the intermittently powered ones, 1.8-7× higher event detection accuracy, experience 50% fewer power failures, and are 44% more available than the sensors that maintain a constant duty-cycle.

KEYWORDS

Energy-harvesting System Design, Dynamic Power Management

1 INTRODUCTION

The ubiquitous vision of the Internet-of-Things is greatly hampered by the "battery problem". As reliable power sources like wall power are not always available where IoT devices are deployed, many devices use batteries as their main power source. Batteries, due to their limited cycle count [5, 35], potential long recharge times [32, 47], and hazardous nature [25, 29] have become a less attractive option as a power source for applications that require low maintenance and life-long service. To eliminate these drawbacks, certain ubiquitous applications which previously relied on batteries as their power source, have adopted energy-harvesting power supplies as an alternative. Such applications include building and home automation, smart industrial monitoring, and smart wearable applications. Recent works have even pushed the boundaries of smart sensing by introducing energy-harvesting medical implants [16, 31], wearable activity tracker [28, 42, 46], micro-satellites for space observation [27], and industrial and residential monitoring [1, 9, 14]. Though energy-harvesting systems are making their way into mainstream sensing applications, a vast majority of the commercial off-the-shelf IoT sensors still rely on batteries [10, 20]. Unfortunately, converting a battery-powered application to energy-harvesting is not as straightforward as replacing the battery with a harvester. Harvestable energy is usually very limited, intermittent, and unpredictable which requires special hardware and software support to achieve useful operation [8, 11, 17, 48].

The operating principle of battery-less energy-harvesting applications can be broadly categorized into two approaches: intermittently-powered and energy-neutral. The first category of sensors harvest energy from the environment through solar, RF, thermal, and kinetic sources, store the energy momentarily in a capacitor, operate until the capacitor is depleted, and repeat this cycle continuously, while the latter store energy for future use and regulate the operational frequency of the sensor to ensure that the outgoing energy roughly matches the combined incoming and stored energy. Various designs implement these techniques to realize energy-harvesting systems, including hardware-based [12, 18, 24, 49] and software-based solutions [7, 11, 26, 36]. In both cases, however, energy-harvesting systems typically consist of a single processor along with an energy-harvesting front-end and application peripherals, where the processor is responsible for both energy management tasks (i.e. tracking the amount of energy stored, controlling the wake-up time interval, turning on peripherals at specific voltage levels, etc.), and application-specific tasks (i.e. sampling, computation, and transmitting radio packets). While this monolithic architecture can be simple and efficient for the intended application, adopting these platforms to build new applications can be quite difficult due to tightly-coupled implementations of energy-management code and application code. The intertwined application and energy management requires the developer to be responsible for understanding not only how to manage energy and correctly implement the application, but also how the two halves might interact.

978-1-6654-9624-7/22/$31.00 ©2022 IEEE
DOI 10.1109/IPSN54338.2022.00033

This tight coupling of energy management and application logic imposes a major limiting factor for energy-harvesting system design. In this paper, we propose Altair, a modular architecture for energy-harvesting system design that decouples energy management from application execution. We claim that traditional power supply interfaces (consisting only of one or more voltage rails and possibly a power available flag) must expand to allow energy-harvesting power supplies to encapsulate the complex energy management tasks required of sophisticated energy-harvesting systems to achieve energy-neutral operation. By requiring the power supply itself to handle tasks including energy forecasting, allocation, measurement, and management, the application logic no longer has to integrate these tasks. Application platforms can focus on the IoT task (as they would with a battery-based power supply), and the new "smart" power supply can make intelligent decisions about when the application should wake up, what operating mode it should be in, and how long it should stay active, based on its careful knowledge of the energy state.

To make these decisions, the Altair design incorporates an energy supervisor that runs energy management protocols (for example, reinforcement-based learning algorithms for harvesting prediction and long-term optimizations for energy neutrality) on behalf of the application. Since the algorithms and power supply are tightly coupled, they can be highly optimized, and must only be implemented once. Many application-level platforms can leverage the same power supply. Further, the energy supervisor can handle the uncertainty in energy-harvesting system deployment, relieving each application from needing to consider the range of potential deployment conditions it might face, and instead allowing the power supply to adapt to the local conditions post deployment.

Expanding the role of the power supply also requires fundamentally re-thinking the interface between the application processor and the energy supervisor. Altair includes a much richer interface that supports a range of potential application platforms. Altair supports "harvesting-aware" applications that can instead use the power supply almost as a co-processor to provide hints about the correct operating mode to use to meet the application's overall operational goals. By supporting a range of use cases, Altair can help many IoT devices embrace the benefits of energy-harvesting operation.

While implementing Altair architecture, we ensure minimal resource conflict on the application hardware by offloading the energy management algorithm to a power-optimized microcontroller. Using a separate core also allows decoupling in the time and power domain and flexibility to be re-used across a variety of devices. To realize Altair design and evaluate its extensibility, we create a prototype implementation of the platform with a functional power supply interface. To demonstrate a potential complex energy management algorithm, we implement a lightweight reinforcement learning (RL)-based duty cycle adaption technique that can run entirely inside the power supply. We provide a bus-based power supply interface, as well as a software library that application platforms can use to interface with the power supply.

In our experiments, we integrate six IoT sensors with the Altair power supply and compare the performance of a variety of energy supervisor control algorithms. By demonstrating the performance of several energy-management techniques on a single hardware platform, integrated with a number of existing devices, we show the generality, flexibility, and robustness of the energy supervisor architecture. Our results show that the event capture rate of sensors when optimized by the RL-based Altair energy supervisor is comparable to using a traditional reliable power source, and the capture rate is 10× higher compared to the intermittently powered ones. Sensors can achieve 1.8-7× higher event detection accuracy with opportunistic duty-cycling. We also find that our system incurs 50% fewer power failures and has 44% more availability than the statically duty-cycled sensors.

To summarize, the main contributions of the paper include:

- We propose, Altair, an energy supervisor architecture for IoT sensing applications that executes energy management decisions separately from the application. We claim that this separation is crucial for better energy optimization and independent application design of energy-harvesting battery-less devices.
- We propose a new power supply-application interface that supports building on top of unreliable power sources and implement a flexible software library to demonstrate the efficiency of the proposed system.
- We implement the proposed architecture as a standalone PCB that can be easily incorporated into new as well as already existing battery-powered devices. The platform is open source.

2 SYSTEM DESIGN CHALLENGES

Energy-harvesting devices must balance an unreliable source of energy with application-level goals. Coupling an application's task flow to an unreliable source of energy makes energy-harvesting systems difficult to develop and debug, and can result in poor performance. Often, the application's task i.e., sensing, computing, or transmitting, is carefully mapped to the recent energy state of the energy storage. This tight integration between an application's task flow and energy availability significantly limits today's battery-less systems in several ways.

Suboptimal performance. With a high degree of energy-application coupling, an application's execution becomes highly energy-dependent. With unreliable energy, the application needs to perform complex software checkpointing techniques to ensure forward progress, which is not always guaranteed. Application programs can enter an endless inactive loop [30, 36], producing suboptimal performance. The complexity, uncertainty, and software overhead induced in intermittent computing indicate a need for alternative approaches to design energy-harvesting systems.

Runtime energy optimization. When an application's task execution is directly mapped to its energy status, this mapping is often performed at design time and is not optimized or re-evaluated during runtime. Decisions made at design time fail to scale post deployment. Since the nature of harvestable energy is time, space, and source dependent, modeling accurate energy states for all possible scenarios apriori is non-trivial. Figure 1 shows two co-located intermittently-powered solar energy-harvesting nodes that both transmit a radio packet each time their capacitor reaches a certain voltage. Though deployed in relatively similar environments, the harvesting rate of the sensors varies quite significantly resulting in different throughput and availability, which is hard to model at design time. Non-linear device parameters are another source of

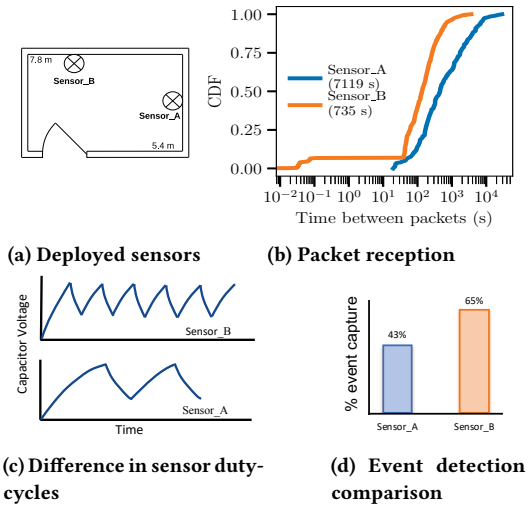

(a) Deployed sensors (b) Packet reception

(c) Difference in sensor duty-cycles (d) Event detection comparison

Figure 1: Two energy-harvesting sensors in room a) transmit at a rate shown in b). Performance varies significantly indicating high energy variability of indoor solar energy. Different duty cycles in c) result in different event detection percentage in d).

stochasticity in energy-harvesting design. For example, two sensors deployed nearby and powered by the same PV cell could operate at different points on its PV curve at a given time and therefore, produce different output power. Different output power results in different capacitor recharge times. Both of these two relations are stochastic and non-linear and fixed design time decisions produce suboptimal performance in post-deployment phases indicating the importance of runtime energy modeling.

Impedes development. Developing applications with unstable power requires more expertise, development time, and rigorous testing and debugging than with reliable power. With the application's behavior being energy-coupled, developers have to carefully implement everything from the low-level energy-harvesting hardware circuitry to writing optimized code within the system's limited energy budget. This creates a large burden on an IoT application developer. Moreover, finding the optimal design strategy often takes multiple design-test-deployment cycles. Successful and smooth battery-less development requires a well-balance between providing enough abstraction as well as control into the underlying energy optimization mechanism [38].

This combination of challenges suggests that a different design architecture for energy-harvesting is required.

3 OVERVIEW OF ALTAIR

We propose Altair, a new energy-management architecture for energy-harvesting applications that decouples energy related decisions from an embedded application's task execution. This separation introduces an abstraction layer between the application and power management which enables independent, modular, and faster design of both subsystems. Altair hides the low-level complexity of energy measurement and management from an application developer, while exposing critical energy parameters through the Altair energy API.

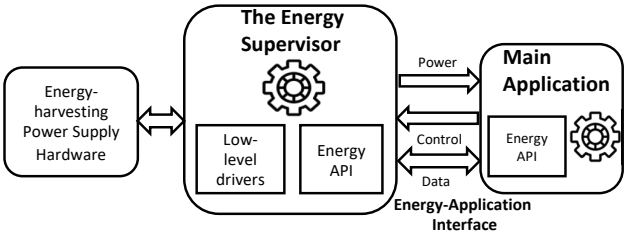

Figure 2: Overview of Altair energy supervisor architecture.

Figure 2 depicts the high-level overview of the Altair energy supervisor architecture. The design consists of three core components: the energy supervisor, the energy-application interface, and the main application. The energy supervisor monitors the energy states of the storage along with load energy consumption and determines the optimal duty-cycle to achieve energy-neutral operation within the limited energy budget. The supervisor works as a wrapper function that implements power supply functionality and an interface to facilitate calls between the supervisor functions and main application. The main application implements the application specific tasks of an IoT sensor such as sampling, computation, and data communication, and makes call into the energy supervisor using the interface. The energy-application interface handles requests from the main application, defines the function-specific input/output parameters, and ensures reliable data communication. Algorithm 1 outlines how the application and the supervisor can interact. The function MAIN invokes ENERGY_SUPERVISOR specifying application requirements ($p_1, p_2, ..$) to receive the rate at which a task is performed. Instead of tying an application's task with the specific energy status of the storage as done in many battery-less applications, the main application offloads the decision to determine an optimal wake-up rate of the sensor to the energy supervisor. This way, the dependence between the energy supervisor and the application is reduced.

3.1 Enabled Properties

Altair enables several desired properties of energy-harvesting system design that traditional implementations often cannot. It introduces a general, reusable, and reliable application-power supply interface for energy-harvesting applications and achieves independent and modular design. Since the energy supervisor and the main application are separate modules of code and the application's task flow is not directly logically dependent on the outcomes of the supervisor, development can be performed in a parallel fashion. This decoupling also simplifies adding new APIs to the energy-supervisor and new functionality in the application. A standard interface between the energy-harvesting power supply hardware and the IoT sensor enables integrating a variety of sensors with a single power supply without re-designing the harvesting circuity or energy management logic, enabling reusability and scalability of the platform. Also, since the application does not interact with the underlying energy-harvesting power supply hardware, the IoT application developer does not need to implement power-supply specific drivers in the application code. Moreover, though we propose Altair for energy-harvesting applications, the general architecture can be adopted in battery-powered IoT and mobile applications as well as for advanced power optimization.

Algorithm 1

```
function ENERGY_SUPERVISOR (p_1, p_2, .., p_n)
    return action_rate
function APP_ROUTINE (rate), // application task code
    return
function MAIN
    After each t_period {
        rate = ENERGY_SUPERVISOR (p_1, p_2, .., p_n)
        APP_ROUTINE (rate) }
```

4 ALTAIR SYSTEM DESIGN

An IoT application interfaces with the energy supervisor of Altair to maximize its energy utilization. In this section, we discuss the core components of the architecture and how they interact. We also investigate the design choices to understand the trade-offs in the design space.

4.1 Design Space Trade-off

We note that the isolation between the energy management and application sub-blocks proposed by Altair can be implemented in both software and hardware. In software, this isolation would be possible by delegating the energy management portion in a separate module with the implementation of appropriate interface functions accessed by the main application. In the hardware version, the energy management functionality could be executed in a separate core or a processor with dedicated hardware resources. We identify some crucial factors when choosing between these various design points. While implementing Altair as a software component would provide the desired logic detanglement and independent code development, we advocate for the hardware version of Altair design to take advantage of several benefits.

4.1.1 Minimal resource conflict. Today's IoT devices are extremely resource-constrained due to their size and power restrictions, yet, they are expected to perform a diverse range of processing-intensive applications. Such applications include critical real-time processing, multi-radio wireless communications, and even running machine learning inferences. Typically these computation-intensive tasks are handled in real-time by a low-end microcontroller causing significant burden on the shared memory and CPU bandwidth. Adding an online energy management algorithm would exacerbate these concerns. Instead, we leverage an ultra-low power microcontroller with dedicated clock, memory, and I/O bandwidth to execute the energy supervisor in parallel with the application.

4.1.2 Decoupling in the power domain. Using hardware isolation and adding additional hardware components to the system might impose an additional energy cost in an energy-harvesting application. However, we argue that the average energy overhead can actually be reduced by leveraging a lower power core than the main application. As these two cores are decoupled in the power domain and they can be turned on/off independently, one can reduce the overall energy cost. This architecture has been implemented by silicon vendors in many low power dual-core processors [43, 45]. Furthermore, the energy-management core can be further power-optimized with the recent growth of ultra-low power chip technology.

Table 1: List of Altair APIs.

Energy Supervisor	Main Application
c_param_t *get_critical_parameters()*	dc_t *get_optimal_dutycycle()*
list_param_t *get_app_list()*	double *get_current_energy_status()*
mode_param_t *get_power_modes()*	int *get_update_period()*
	model_array_t *get_energy_model()*

4.1.3 Reusability and generality. A hardware implementation of Altair accelerates the development phase and reduces developer effort by providing modularity and reusability across multiple applications. To promote reusability, we adopt the hardware-accelerated software energy management of Altair and implement the energy supervisor in a lower power microcontroller taking inspiration from the ARM's big.LITTLE technology [4] that leverages a smaller lower power core to enable power optimization. In the evaluation, we test the performance with a variety of IoT sensors and demonstrate the composability and generality of the platform. This enables future embedded designers to rapidly develop their own applications while adopting energy-harvesting functionality.

4.2 The Energy Supervisor

The energy supervisor of Altair handles the tasks of energy management, prediction, and allocation, and makes decisions independently from the application logic. To accomplish this, the energy supervisor has two key components. First, the supervisor interacts with an energy-harvesting front-end to collect useful information about the harvesting conditions. This information includes the average input power, the charging rate of the storage, and instantaneous and average stored energy. The energy-harvesting front-end typically accommodates an energy-harvester (e.g. solar, RF, thermal, or piezoelectricity), a charge controller, and an energy storage (e.g. capacitor). Second, the supervisor implements the dynamic power management scheme and the interface presented to the main application. For dynamic energy management, the application can specify the parameters (i.e., duty-cycle) to be optimized and an optimization algorithm among the supported ones. The supervisor can also inform the application about which operating mode the application peripherals should be running in, or the recommended order of priorities for multiple applications.

The supervisor makes power management decisions by keeping track of system's past experience and predicting future expected energy incomes. Learning and adapting the optimization parameters at runtime, as opposed to fixed design time or datasheet parameters, makes the energy supervisor more robust to real-world deployment conditions. The supervisor attempts to support any type of application workload. However, as the underlying hardware can only buffer a finite amount of energy, the average energy consumption of the application must be below the maximum buffered energy.

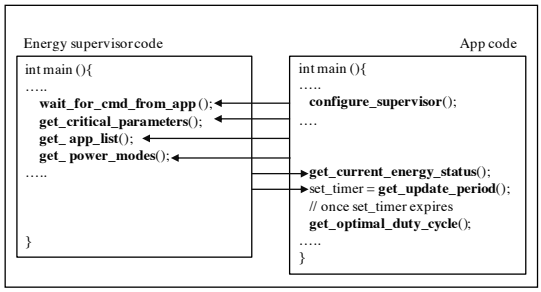

Figure 3: Example workflow diagram between the application and energy supervisor. The direction of the arrow specifies the direction of API calls.

4.3 Energy-Application Interface

The energy-application interface enables the abstraction layer between the main application and the energy supervisor module. It facilitates communication between the energy supervisor and the main application by implementing a set of useful APIs. This standard interface enables updates and improvements to the energy supervisor and any optimization algorithms without requiring direct changes in the application.

4.3.1 Altair Energy API. Table 1 shows the list of available APIs provided by Altair. The energy supervisor calls *get_critical_parameters*, *get_app_list*, and *get_power_modes* to acquire application or device specific information. These are fixed configuration parameters of the application that are not expected to change at runtime. *get_critical_parameters* returns an array of permitted duty-cycles of the running application, according to which the energy supervisor optimizes for long term energy neutrality, and which energy optimization algorithm from the supported ones to use. Currently, the platform implements three duty-cycling mechanisms (described in Section 6.2). To understand how energy is being spent, *get_app_list* provides the list of energy-atomic operations performed by the application. Energy-atomic operations are categorized into sampling a sensor, computing and analysing the sampled data, transmitting data, or receiving data. Each of these operations is associated with a unique operation ID. The application specifies the required operating power modes using *get_power_modes*. Altair saves this information into the non-volatile memory of the energy supervisor to eliminate the need to repeat the APIs calls after a power failure.

On the application side, Altair provides another four APIs, namely *get_current_energy_status*, *get_optimal_dutycycle*, *get_update_period*, and *get_energy_model*. *get_optimal_dutycycle* returns the calculated optimal duty-cycle which is one of the values specified by *get_critical_parameters* and the power modes of each operation. The application performs sensor sampling, computation, and communication at this optimal rate and enters sleep mode in between operations. The *get_update_period* returns at what interval the application should check for the updated duty-cycle. This depends on how variable the incoming energy profile of the device is (defaults to 15 minutes). The *get_current_energy_status* and *get_energy_model* offer finer insight into the system's energy status. By calling these, the application receives the current stored energy on the capacitor and the current numeric input values used by the duty-cycle algorithm to calculate the duty-cycle, respectively.

4.3.2 Hardware Energy Interface. The hardware energy interface consists of the hardware abstraction layer that configures the hardware interface between the supervisor and the application. Each API call is executed by a set of hardware signals and a data communication channel. The interface consists of voltage, control, and data channel as shown in Figure 2. The data channel enables a synchronous communication channel between two processors where the application processor provides the clock signal. When the application processor makes a call into the API functions, it sends an interrupt signal to the energy processor. The energy processor uses the interrupt to configure the communication hardware and initiate data transfer. The energy API calls described in the previous section are translated into data packets. The first byte of energy API packet encapsulates header information specifying the intended API call and a read/write bit, and the next two bytes specify the message length. To invoke the energy supervisor to call an API, the main application sends a write request and an API call from the application is sent as a read request. Both processors avoid sending a new request if there is any previous unresolved or pending request. We also keep a timeout timer to avoid a communication deadlock.

Figure 3 shows a flow diagram between the energy supervisor and the application code using Altair energy API. Upon startup, the main application uses the *configure_supervisor* to send write requests and prompt the energy supervisor to call the next three functions for configuration. *get_current_energy_status* and *get_energy_model* is called at any time application, while, the *get_optimal_dutycycle* is invoked according to *get_update_period*.

4.4 The Main Application

The main application is a piece of software that performs the typical workload of an IoT sensor, i.e. sampling, computing, processing, and transmitting.

5 ALTAIR PLATFORM IMPLEMENTATION

We implement the Altair energy-harvesting power supply module in a custom PCB.

5.1 Hardware Components

The Altair hardware consists of two primary modules: a power system module and an external application module. The power system module implements the energy supervisor, low level energy-harvesting hardware, and the hardware interface between the energy supervisor and the main application. The main application is representative of a typical IoT sensing application that is powered through the power supply interface.

Power supply module. The power supply module of Altair hardware accommodates an energy-harvesting front-end and a companion microcontroller that implements the energy supervisor software. Figure 4 shows the power supply module and the block diagram of the core components.

An ultra-low power battery charger IC SPV1050 charges the supercapacitor from a solar or TEG harvester until it reaches 3.1 V. A nano-power boost regulator MAX17222 with > 70% efficiency at 10 µA of input current regulates the supercapacitor voltage after its voltage reaches 2 V. The platform currently uses a monocrystalline IXYS solar cell as the harvester and a 470 mF supercapacitor

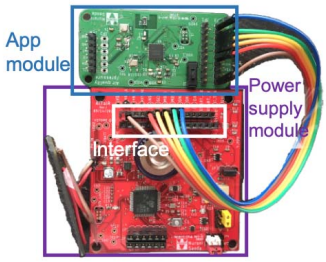

(a) Altair Power supply board interfacing with a sensor.

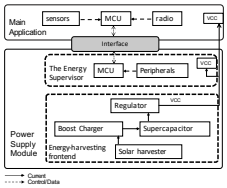

(b) Hardware block diagram.

Figure 4: The Altair hardware platform consists of a power supply module that implements the energy supervisor and a discrete power supply application interface that can be plugged in directly with an external application.

with an ESR value of 25 Ω as electrical storage. We size the capacitor empirically to ensure that it can supply the highest system peak current.

The energy supervisor uses an ultra-low power 32-bit ARM Cortex-M0+ with a 8 kB of SRAM and 64 kB of flash with different low power modes. The power supply consists of a current-sense amplifier MAX9634 to keep track of the load energy consumption. A nano-power power gating IC TPL5110 with reconfigurable time interval allows the MCU to duty cycle the application in hardware with minimal calibration. The MCU leverages a digital potentiometer to dynamically reconfigure the time interval according to the calculated duty cycle.

The interface. The interface of the power supply module provides two voltage rails of 3.3 V and 1.8 V, one duty-cycled voltage rail, capacitor voltage output. We use SPI to exchange information between the two microcontrollers and one GPIO to trigger interrupts. For debugging and evaluation, the interface exposes a UART channel that can be used to log the instantaneous capacitor voltage state and current measurement channel.

Application module. The application module of Altair platform is an externally attached sensor. We implement an air quality and pressure sensor board as a part of the platform.

5.2 Energy Supervisor Implementation

We implement an example energy supervisor to show how the architecture can be leveraged to optimize the duty-cycle of the connected application. With the dedicated hardware resources of the energy supervisor microcontroller, processing-intensive on-device energy optimization can be implemented without imposing significant resource conflict on the application microcontroller. One of the useful properties of the energy supervisor is its capability to learn to behave optimally post deployment without explicitly modeling the harvesting environment pre-deployment. To demonstrate this, we implement an on-device energy supervisor using reinforcement learning. Reinforcement learning has shown promising results as a power management technique since it can enable the sensor node to learn to adjust its duty cycle in a completely unknown environment [3, 21, 41]. The RL-based energy supervisor reacts to changes in available energy to update an application's operation, in this

Algorithm 2 RL Algorithm for Energy Management

Initialize S, A, $Q(s,a) = 0$, α, γ, ϵ , δ
while true **do**
  for each episode **do**
    $s \leftarrow$ Sample current states
    $a \leftarrow$ Choose current action from s using ϵ-greedy policy
    wait for a duration of t_{wait}
    for each step of the episode **do**
      Perform action a for the duration of t_{step}
      wait for a duration of t_{wait}
      $s' \leftarrow$ Sample next states
      $r \leftarrow$ reward (s', a) according to equation (3)
      $a' \leftarrow$ Choose next action using ϵ-greedy policy
      $Q(s,a) \leftarrow Q(s,a) + \alpha * [r + \gamma * (Q(s'), a') - Q(s,a)]$
      $\epsilon \leftarrow \epsilon - \delta$
      $s \leftarrow s'$
      $a \leftarrow a'$

implementation, the rate of sending packets to report an event. The goal of the algorithm is to maximize the application sensing rate while avoiding critical energy depletion.

At a given time, the energy-harvesting node acts as an agent in different states ($s_t \in S$) corresponding to the available stored energy, incoming energy, and energy consumed by the load. The environment in this scenario consists of the stochastic harvestable energy source and the randomness inherent in the sensor hardware. The node interacts with the environment in time-slotted episodes by selecting a sensing rate ($a_t \in A$), and receives feedback in the form of reward ($R : S \times A \rightarrow R$). Through a series of such interactions with the environment, the agent finds its optimal policy ($\pi*$) to select future actions.

RL algorithm. We define the state space for the algorithm to capture the energy profile of the system. At a given time-step t_k of an episode, the energy supervisor collects all the following state information,

$$S = \{e_{st}(t_k), e_{in}(t_k), e_{load}(t_k)\} \tag{1}$$

where $e_{st}(t_k)$, $e_{in}(t_k)$, and $e_{load}(t_k)$ denotes the supercapacitor voltage at t_k, average input energy, and the load energy consumption during t_k. These parameters are indicative of the system's overall energy dynamics for which the supervisor finds an optimal action for the sensor. We consider a 24-hour long episode with a time step of 20 minutes.

The action space consists of a set of discrete sensing rate,

$$A = [r_{min}, ..., r_{max}] \tag{2}$$

where r_{min} and r_{max} are the minimum and maximum rate for the application. At each time step t_k, the agent selects an action $a(t_k) \in A$ according to the underlying policy. The goal of the reward function is to inspire the agent to choose the actions that maximize the sensing rate of the application and maintains minimum required energy on the energy storage. To model the reward function we adapt the reward function proposed by Aoudia, et al. [3] as follows:

$$R = (e_{st} - e_{min})/(e_{max} - e_{min}) * a(t_k) \tag{3}$$

We assign a negative reward of -400 if capacitor voltage falls below the minimum required voltage level of 2.0 V. We choose this number so that the maximum cumulative reward over an episode

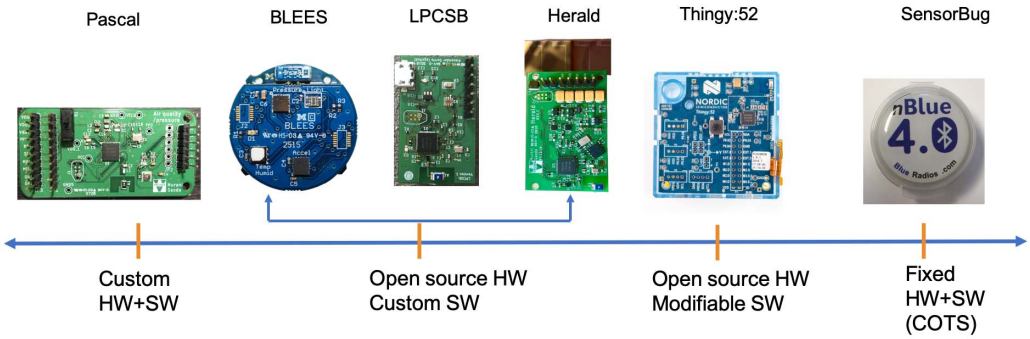

Figure 5: Spectrum of IoT sensors on a scale of hardware and software flexibility. The left-most category has maximum flexibility, whereas to the right-most has fixed hardware and software. We evaluate the ALTAIR platform with different points on this scale to demonstrate generality.

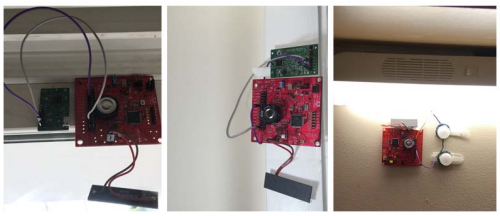

Figure 6: ALTAIR device deployments.

does not exceed the negative reward. Algorithm 2 lists the pseudocode showing how we implement the SARSA reinforcement learning technique [44] to calculate the optimum duty cycle of an application.

Parameter setup. Though states and actions are continuous functions, we discretize those to restrict the size of Q-matrix. The discrete action space is A = [1,2,3,4,5] s, which denotes the time between two consecutive tasks. We set $\lambda = .99, \gamma = .8, \lambda_{min} = .1, \delta = .001, \alpha = .1$ after explicit testing. To enable faster convergence, we ensure that the learned Q-table is saved before a power failure happens by polling the capacitor voltage in the background.

6 EVALUATION

To evaluate the ALTAIR design, we investigate the usability of the energy supervisor architecture and develop a set of different IoT applications. To demonstrate the versatility of the architecture, we run the applications using different energy supervisor algorithms and compare their performance. We tested the platforms across four categories of IoT hardware and evaluated how well these applications perform in terms of event generation frequency for periodic sensing and percentage of accurate detection for event-based applications. We integrated six sensors with the ALTAIR hardware platform. We also explore the performance of the reinforcement learning based energy supervisor to understand how well the system adapts in terms of cumulative active time and reactivity—an inherent feature of the energy supervisor that shows the online adaptability of the system in post deployment situations.

6.1 Methodology

Categorizing existing IoT devices. ALTAIR uses its standard hardware and software interface to enable different applications. To test the usability of the ALTAIR power supply interface, we broadly categorize existing IoT devices into four groups based on the hardware and software interface exposed by the device: 1) sensors that are custom built specifically to use with ALTAIR platform ensuring ideal interfacing, 2) sensors with open source hardware and optimized applications, 3) sensors that have available hardware design with somewhat modifiable software stacks, 4) off-the-shelf sensors with non-modifiable hardware and software. This spectrum is shown in Figure 5. Of these four groups, the first group of sensors is best suited for use with ALTAIR. However, embedded software developers typically use the second and third categories of sensors.

We select six IoT sensors from these four categories to perform our experiments. These sensors are 1) a Pascal sensor board that

Test platforms	Processor	Peak current (mA)	Default power supply	Available interface
Pascal	Cortex-M4 nRF52840	13.6	flexible	power supply, SPI
BLEES	Cortex-M0 nRF51822	15	Non-rechargable battery	power supply
Herald	Cortex-M0 nRF51822	14.8	Intermittently powered	power supply
LPCSB	Cortex-M0 nRF51822	14.6	USB-powered	power supply, I2C
Nordic Thingy:52	Cortex-M0 nRF52832	10	Rechargable battery	power supply, I2C, SPI, MOSFET drivers, IO
SensorBug	BR-LE4.0-S3A	17	Non-rechargable battery	power supply

Table 2: Specifications of test applications.

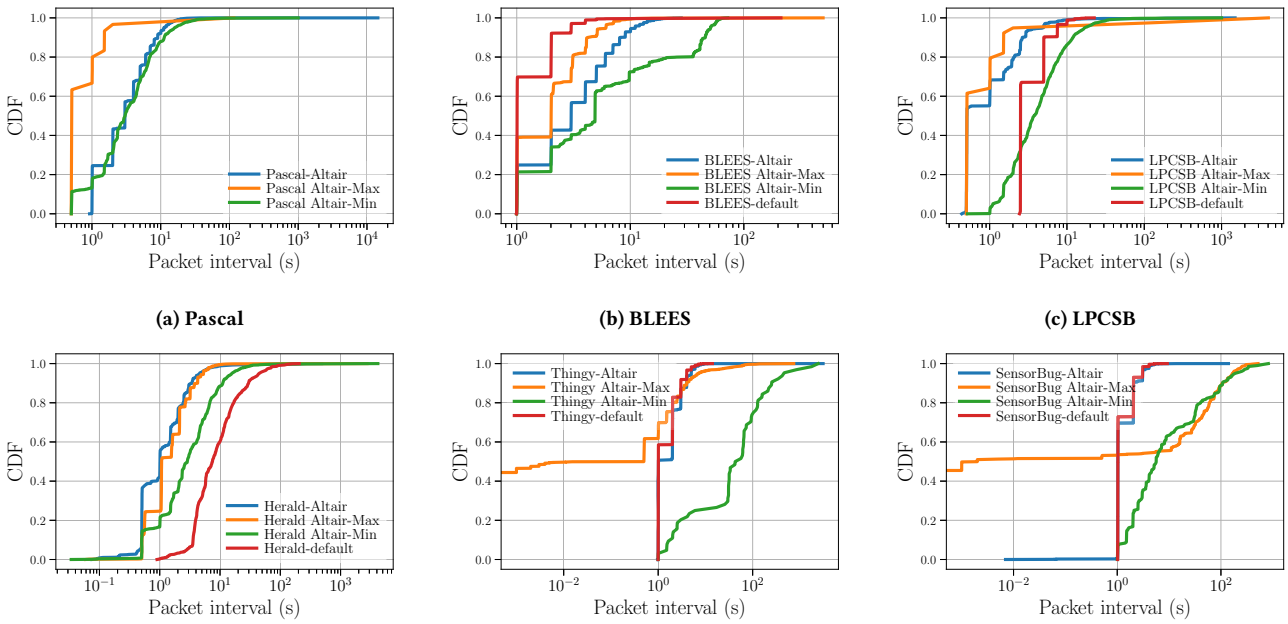

(a) Pascal **(b) BLEES** **(c) LPCSB**

(d) Herald **(e) Thingy** **(f) SensorBug**

Figure 7: Performance of different sensors when optimized by different variants of the energy supervisor and their default power supply. The Altair energy supervisor implements reinforcement learning to choose between a set of transmission intervals. BLEES, LPCSB, and Thingy:52 sensors using Altair produce a similar distribution of packet frequencies as the continuously powered version. For intermittently-powered Herald beacons however, Altair produces denser packet distribution.

monitors ambient air quality and pressure (category 1), 2) the BLEES platform [1] that senses temperature, humidity, light, pressure, and movement, (category 2), 3) the LPCSB [40], an ambient light sensor that categorizes natural light from sunlight, (category 2), 4) Herald, an intermittently-powered energy harvesting Bluetooth Low Energy (BLE) beacon [39] (category 2), 5) the Nordic Thingy:52 [33], a multi-sensor prototyping platform (category 3), and 6) the SensorBug [6], a BLE beacon for smart home monitoring with temperature, light, and acceleration sensors (category 4). While BLEES, LPCSB, Herald hardware have limited hardware interfaces, the Pascal and Thingy platform includes a relatively richer interface with ports for communication including I2C and SPI. For the devices that do not have a data channel or open software that we can reprogram, we use the duty-cycled voltage terminal of the power supply interface to turn on/off the sensor according to the calculated duty-cycle. This exhibits the benefit of using the hardware version of the energy supervisor as discussed in Section 4.1.3.

The selected devices are designed to work on different powering options including rechargeable/non-rechargeable batteries, constant power, and intermittent source of energy. Also, these sensors use different application microcontrollers and their energy consumption varies. Table 2 lists the characteristics of these hardware platforms. Altair's strength lies in its ability to take a battery-powered sensor and convert it to a self-powered energy-harvesting device. We envision that this will pave the way to many future battery-less applications.

Interfacing with Altair. To interface with Altair, we simply deactivate the default power supply of the sensor and jumper the power rails and SPI channel to the Altair power supply. In the Thingy:52 board, we connect the voltage rails bypassing the battery monitoring circuitry. The application uses the energy API library at runtime to interface with the energy supervisor. The application developer implements the mapping between the API and their corresponding request id as an initial configuration for both the application and energy supervisor.

Sensing applications. We consider periodic and event-based sensing tasks from the above four categories to understand how well the adaptive power management algorithm captures useful events. The sensors use Bluetooth Low Energy (BLE) radio to report events. An always-on BLE receiver scans for advertisement packets and advertisements are sent with short intervals in between, in the range of milliseconds to a few seconds.

Deployment. Our deployment scenario consists of four different indoor locations in a building space that are exposed to variable light levels across different times of a day: on three walls, on a desk, a door, and a window. Figure 6 shows some of the deployed devices. A gateway device collects the BLE packets sent by the deployed sensors and logs them for post-processing. We train the energy supervisor reinforcement learning agent before beginning the data collection unless specified otherwise.

6.2 Energy Supervisor Performance

Event frequency. In this section, we compare the performance of the six test sensors in terms of the captured event frequency with respect to their default power source and different variants of

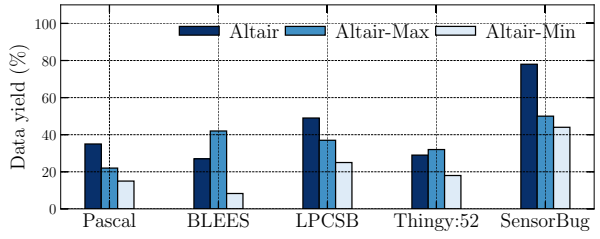

Figure 8: The percentage data yield of each sensor normalized to their default power supply. The ALTAIR energy supervisor produces better data yield than the Altair-max variant that always selects the high sampling rate.

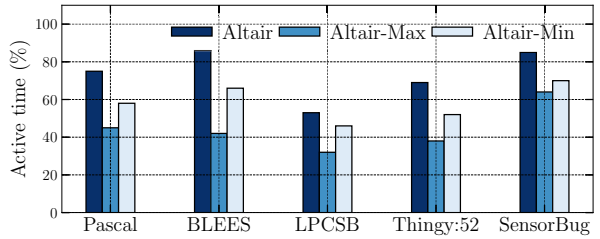

Figure 9: Percentage active time comparison across different energy supervisors. Active time denotes the percentage of time within an interval the sensor was continuously transmitting data. Altair outperforms the other variants.

the energy supervisor running on the power supply. The different variants of the energy supervisors are: Altair that runs the energy supervisor as discussed in Section 5.2, Altair-Min which always chooses the minimum duty cycle, hence maximum delay between packets (5s), and Altair-Max which chooses the minimum delay between packets (1s). We evaluate the cumulative distribution function (CDF) of the time between packets received by the receiver. Figure 7 compares the results. The time between two consecutive samples is a helpful parameter to understand overall how responsive the system is to an external event. The denser the samples, the more likely is the system to report critical events.

The sensor workload consists of taking a sample and reporting the data in BLE packet. When powered with the default supply, we program the BLEES, LPCSB, Thingy:52 sensor to send a BLE packet with the sensor data every second and SensorBug has a pre-programmed advertising interval of 1636 ms. For the herald beacon, however, the rate at which a packet is sent is proportional to its rate of harvesting energy. When connected to the ALTAIR power supply, the sensors dynamically change the packet sent rate reacting to the changes in available energy.

We observe from the distributions of packet intervals in Figure 7 that for BLEES, LPCSB, and Thingy:52 sensors, the distribution curve of ALTAIR and the default power supply follow closely, and the 95th percentile of the inter-packet times are within ten seconds. The SensorBug, in contrast, achieves 111 s. The packet interval distribution of SensorBug with ALTAIR follows similar pattern as the default power, however, it undergoes longer occasional power

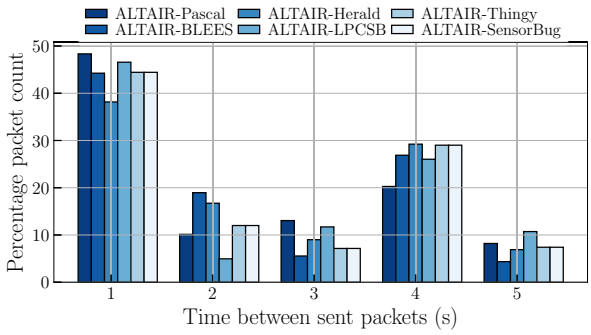

Figure 10: Packet distribution with ALTAIR. Sensors with ALTAIR opportunistically choose between five allowable rates, prioritizing the higher rate.

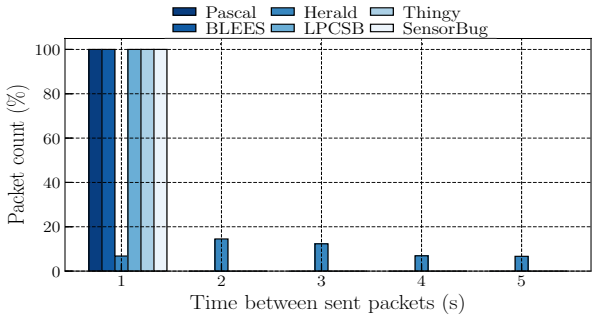

Figure 11: Packet distribution with the default power source.

outages due to its relatively high peak current (Table 2). ALTAIR achieves overall higher captured event frequency than Altair-Min, the intermittent power supply, but worse than Altair-Max. For the intermittently-powered herald beacons, the time between consecutive samples is directly affected by the availability of harvestable energy and charge time of the storage capacitors resulting in larger delays. ALTAIR system however masks the irregularity of energy by storing it in a sufficiently sized capacitor and ensures samples are collected evenly at the desired rate. According to Figure 7, Herald achieves 10× higher captured event frequency with ALTAIR than with its intermittent power supply.

ALTAIR produces better percentage data yield and active time than both baselines as shown in Figure 8 and Figure 9, as ALTAIR optimizes for better sensing rate and fewer power failures. The percentage data yield signifies the amount of produced data normalized with respect to constant power sources and the percentage active time denotes the time in a fixed time interval for how long the sensor was active.

Figure 10 compares the distribution of inter-sample times of the sent packets. ALTAIR distributes the sample rate among the allowable rates reactively based on the decision of the energy supervisor. The RL agent chooses more and more actions that sample packets at a high rate when there is an energy surplus and relaxes the rate when the system is likely to see a power outage. The distribution shows that for all the sensors more than 35% of the total samples have a rate of one sample per second. Figure 11 shows the distribution for the default power supply. In the case

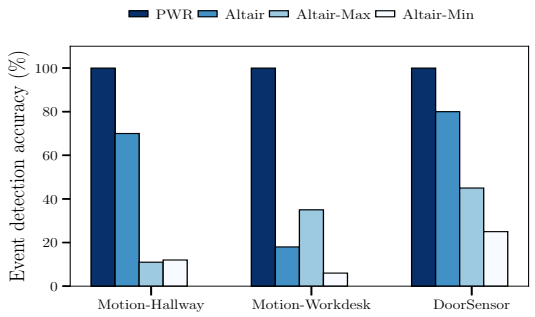

Figure 12: Event detection accuracy for time critical applications.

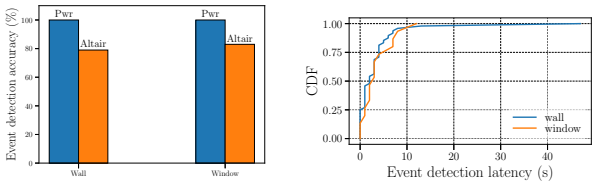

(a) Temperature event detection accuracy. **(b) Event detection latency CDF.**

Figure 13: Non-time critical event detection using Altair.

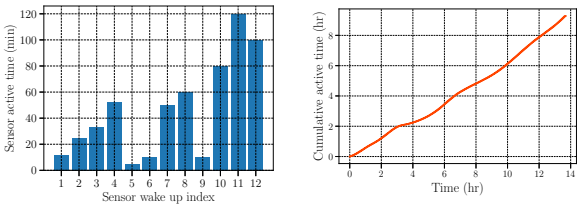

(a) **(b)**

Figure 14: When moved to a new environment, the system increases its activity as it learns the new harvesting conditions.

of intermittently-powered systems, the samples are more sporadic and the sensor is spending majority of the time in charging the energy storage. Such systems are likely to miss events than Altair that prioritizes higher sample rates when possible.

Event detection accuracy. To investigate how well applications can detect external events with Altair, we classify event-based applications into two categories: time critical and non-time critical. For the time critical scenario, detecting an event should be instantaneous (i.e., less than a few seconds) since some external agent might need to react that event, for example, door sensors and motion-based light switch. For the non-time critical applications, detecting an event in a reasonable time interval is sufficient, for example, temperature sensors for HVAC systems. We deployed one BLEES sensor to detect door events, one to detect motion in two different locations and one Thingy:52 to detect temperature events.

We connected one BLEES board with the Altair power supply and deployed it on a door to detect each time the door has been opened or closed, and two of them in a hallway and on a desk to detect movements for one week. With the default power supply, when the sensor gets an interrupt due to an event, BLEES wakes up to report the event. When connected with Altair, the power supply processor fully controls the turn on/off the BLEES application processor. For the Thingy:52 board, the sensor is configured to go to the sleep mode and wake up when an event happens and report that event only if the capacitor has sufficient voltage. We chose to detect motions in two different locations to emulate two real-life scenarios: spaces that are usually lit most of the time of a day like a hallway, and spaces that have sporadic light exposure and sensing and harvesting is likely to happen simultaneously such as at a desk. To ensure we have enough data for statistical reasoning, we expedited the data collection process at the end by manually generating events as capturing organic events takes significant time. We used a constantly powered version of the sensors to collect the ground truth for events. We compared the performance of Altair with two variants: ALTAIR-Min that always chooses minimum duty-cycle and ALTAIR-Max that selects maximum duty-cycle.

Figure 12 shows the percentage of correctly detected events and compares the result across three power management algorithms in three of the deployment scenarios. We find that sensors with Altair achieves 70% and 80% detection accuracy in the hallway and on the door respectively, higher than the other two variants. This happens since Altair spreads out the system active time by optimally choosing the duty-cycle and is likely to capture events correctly, whereas, ALTAIR-Max sees frequent power failure events and ALTAIR-Min misses events for spending much time in time between wake-ups. However, in the work-desk space ALTAIR-min detects more events than Altair as it aggressively selects higher sampling rate. This signifies that careful decisions should be made for applications where the event of interest can happen before the device can harvest enough energy. In such scenarios, predicting such events beforehand can improve detection accuracy. We plan to investigate such cases for future study.

As a candidate of non-time critical event detection, we deployed one Thingy:52 to monitor the temperature of a home in two different locations: on a window and on an indoor wall. We analyze how many times the sensor can correctly report when the temperature falls below 76°F or exceeds 79°F (selected according to the comfort level of the occupants). Figure 13(a) shows that with Altair the device reports 79% and 83% of the events accurately. To determine the latency between the event has occurred and successfully reported, we show the CDF of detection latency in Figure 13(b). We find that the 95th percentile latency remains within 12 s.

6.3 RL Supervisor Robustness

System active time. Altair uses a 470 mF supercapacitor as an energy-reservoir of the system. The larger the size of the capacitor, the more time it takes to recharge after a power failure. In this section, we aim to analyze the active time of a sensor connected to Altair. We define the duration of the time a sensor samples continuously before exhausting its energy buffer as the active time.

To evaluate how much time the system spends in recharging the capacitor in a dynamic energy environment, we moved the

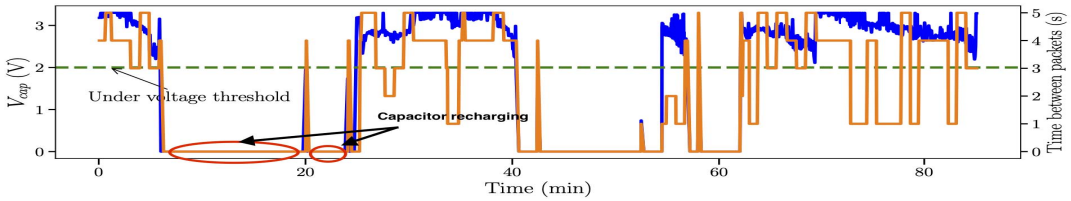

Figure 15: With time, the energy supervisor learns to avoid power failure by adjusting the time between samples, though experiences a few power failures at the beginning. The blue trace plots the instantaneous capacitor voltage, and the orange corresponds to the to the time between packets.

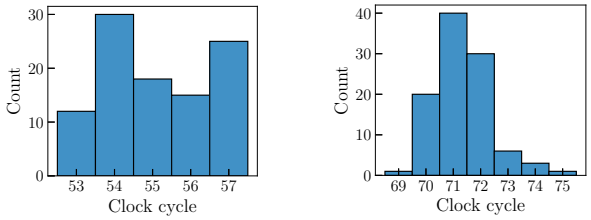

(a) Wake-up delay **(b) Interrupt service delay**

Figure 16: The histogram of the delay in servicing the message request by the energy supervisor in clock cycles.

Thingy:52 sensor from its original window position to a wall. Figure 14(a) shows the active time of the sensor during each progressive power cycle. After being exposed to a new environment with a different harvesting scenario, at first the system explores to find the optimal set of actions that avoids power failure. The system active time progressively increases as it sees less power failures with occasional dips. Figure 14(b) shows the cumulative active time of the sensor.

Reactivity. In this section, we analyze how the energy supervisor reactively changes the rate responding to the available energy. A sensor that runs at a constant duty-cycle suffers from multiple consequences: 1) in case of an energy surplus, the system underperforms by not sampling more, and 2) in case of an energy drought, the system runs the risk of frequent power failures by not backing off. Figure 15 shows how Altair adjusts the time between samples reacting to the capacitor voltage. We set the episode interval as 2 min for this experiment. In the beginning, the system experiences frequent power failures around 8, 15, 22 and 25 minutes, spends significant time in power failure, but learns to adjust the time between samples allowing the sensor to sleep. A falling capacitor voltage results in an increase in the time between samples and a steady or rising capacitor voltage encourages frequent samples. Throughout this experiment, the harvester was kept under a stable harvesting environment which ensures that the capacitor voltage was only the system variable. By vary its rate of operation, the system incurs 50% fewer power failures with an increased availability of 44%.

6.4 Energy Supervisor Responsiveness

As the energy supervisor processor receives the energy API request from the main processor through a hardware GPIO interrupt, we investigate the number of clock cycles needed to serve the interrupt. We characterize the delay to wake up the energy supervisor from a low power sleep and the delay to respond to an interrupt while performing its routine task. We show the histogram of delays of 100 interrupts in Figure 16(a) and Figure 16(b), respectively. Though the delay in terms of clock cycle varies, the distribution shows the delay can be bounded within a few clock cycles.

Table 3: Power draw overhead of Altair.

Component	Active current	Sleep current
MCU STM32L010R8	585 µA@16Mhz	4.7 µA
Charger SPV1050	2.6 µA	1 nA
Current Sensor Max9634	1 µA	1 nA
Power Gating TPL5110	35 nA	N/A

6.5 Energy Overhead

Using the Altair platform does come with an energy overhead. However, while implementing the platform, we chose components with low power options. Table 3 lists the active and sleep current of the used components. The average active power draw of the board is 7.8 mA and the quiescent power draw is 94.5 µA. We notice that the significant energy overhead comes from the ADC polling to observe the system energy as ADC reading over one second costs 24.3 µJ. This overhead can be reduced by polling the ADC less frequently.

7 RELATED WORK

In this section, we review state-of-art designs and architectures in energy harvesting systems and reactive power management schemes using reinforcement learning.

7.1 Energy-Harvesting Device Architectures

Existing works for energy harvesting systems can be broadly categorized into two directions: intermittent systems which perform operations whenever there is enough energy and non-intermittent systems which usually store the harvested energy in larger capacitors for future use.

Intermittent systems are often equipped with small energy buffers and perform simple tasks whenever the stored energy reaches a certain threshold. For example, the Gecko [48] and Monjolo [13] principle performs sense and send type workload whenever the capacitor voltage reaches certain threshold. Monjolo exploits the insight that the rate of energy-harvesting is indicative to the sensed quantity. However such insight fails to scale outside the intended applications since the source of sensing and harvesting are often not co-related. One proposed architecture and toolkit for energy harvesting systems uses a similar principle [9], which masks the inevitable intermittency with a variety of trigger abstractions that

activate the device for certain conditions. With Altair, we advocate for the power supply to be standard across different types of sensing applications.

UFoP [18] introduces the concept of federated energy that charges a dedicated capacitor for each peripheral which is responsible for specific individual tasks. By discarding the idea of a central storage for the whole system, UFoP provides flexibility for each peripheral and promotes modular application development. Flicker [19] further improves modularity and flexibility required for rapid prototyping of battery-less applications by allowing the peripherals to reconfigure their activation thresholds at runtime. Federating energy across multiple energy stores decreases the dependency between the energy availability on a single energy storage and each peripheral's task execution. While being motivated by similar goals of modularity, flexibility, and generality, Altair decouples the energy logic altogether from the application, dedicating a sophisticated hardware module and introducing a novel software interface in the battery-less system design. Altair moves away from the intermittent principle of operation to achieve higher uptime and to support long running applications. Capybara [24] introduces a hardware-software approach to match the energy requirement by a task by dynamically resizing for its banked capacitor, which reduces cold start and capacitor recharge time. It provides the flexibility to choose from different energy modes and a combination of capacitors to activate according to the requirements of the application. While Capybara adopts a task-based model to map each tasks to energy modes and energy modes to the dynamic size of the capacitor, we adopt an interface-based architecture to reduce the direct coupling between the underlying power supply hardware and the application. The signpost platform [2] is a generalized energy-harvesting platform for city-scale sensing using a shared backplane to interconnect and isolate each module, allowing energy to be used for a particular module. In Signpost, applications virtualize the amount of stored energy and employ a different duty-cycling strategy without affecting each other's execution. In Altair, we make the power supply itself programmable which continues to learn and adapt post-deployment to learn new strategies to achieve optimal duty-cycling strategy.

7.2 Dynamic Energy Management using RL

Reinforcement learning (RL) has been adopted for dynamic energy management in energy harvesting nodes. Hsu et al. [22] introduce a dynamic power manager for energy harvesting networks using Q-learning algorithm. Another work provides dynamic throughput provisioning according to the battery's energy level [23]. The RL agent attempts to avoid specific states of the energy storage, which include overcharging, deep-discharge, and depletion. Different from other approaches, Rioual et al. [37] investigate the performance of different reward functions for energy optimization in energy-harvesting IoT nodes. Fraternali et al. [15] introduce a day-by-day learning algorithm using reinforcement learning to maximize the quality of service of the sensing. Another SARSA algorithm proposed by Ortiz et al. [34] attempts to learn a power allocation policy in two-hop communications and maximize the throughput of a communication system. SARSA (λ) was also introduced to develop an adaptive power management algorithm for solar-energy-harvesting nodes [41] using large weather datasets. In this paper, we implemented a SARSA reinforcement learning on a resource-constrained embedded device to maximize the event generation and event detection rates of IoT sensing applications.

8 DISCUSSION

Partial decoupling. Though Altair reduces the logical dependency between energy management and application tasks, both subsystems are required to have a knowledge of the expected information from each other. Since IoT sensors are typically small systems with a handful of running applications, we expect the Altair architecture is sufficient. However, for large scale embedded systems full decoupling may be needed.

Vast heterogeneity of IoT applications. Though we believe that Altair is a stepping stone in the direction of a "general-purpose" energy-harvesting power system suited for IoT sensing applications, the spectrum of sensing is broad in terms of energy cost and time-sensitiveness. Applications that are susceptible to occasional power failures might require back-up source of energy such as rechargeable batteries [24]. In such a case, the RL manager might reduce the negative reward, if the backup energy source is available.

Energy storage size. Though an over-provisioned energy reservoir can mask unstable available energy and eliminate the need for complex software support, bigger capacitors suffer from higher leakage, prolonged cold-start phase, and longer recharge times.

Limited harvester support. Current Altair platform only has support for harvesting energy using solar and TEG harvesters.

Enabling new techniques. We believe that faster testing and development plays an important factor when designing novel energy-harvesting applications and Altair attempts to lower the barrier to entry. We recognize that there is a lack of prototyping platform for energy-harvesting application and this work will attract researchers to build and test new software and hardware techniques for better power management.

9 CONCLUSION

Managing energy is critical for energy-harvesting systems, and this burden has been foisted on the IoT application software with only limited support from the energy-related hardware. We argue that ad-hoc and implementation-specific interfaces between applications and power supplies constrain the development of energy-harvesting devices, and that a new MCU-power supply interface is critical for restoring proper layering to these systems. In this paper, we introduce such a system that isolates the energy management decisions from a sensor's workload, and provides a simple interface for adding new applications to the system. By strictly separating energy-management from device operation, we believe we can lower the bar for developing energy-harvesting systems, helping to realize a fully batteryless IoT.

10 ACKNOWLEDGEMENTS

We thank the anonymous reviewers and our shepherd for their valuable insights and feedback on improving this paper. This work is supported in part by the National Science Foundation (NSF) under grants CNS-1823325 and CNS-2144940, and the Strategic Investment Fund at the University of Virginia.

REFERENCES

[1] Joshua Adkins, Bradford Campbell, Samuel DeBruin, Branden Ghena, Benjamin Kempke, Noah Klugman, Ye-sheng Kuo, Deepika Natarajan, Pat Pannuto, Thomas Zachariah, Alan Zhen, and Prabal Dutta. 2015. Demo: Michigan's IoT Toolkit. In *Proceedings of the 13th ACM Conference on Embedded Networked Sensor Systems* (Seoul, South Korea) *(SenSys '15)*. Association for Computing Machinery, New York, NY, USA, 485–486. https://doi.org/10.1145/2809695.2817866

[2] Joshua Adkins, Branden Ghena, Neal Jackson, Pat Pannuto, Samuel Rohrer, Bradford Campbell, and Prabal Dutta. 2018. The signpost platform for city-scale sensing. In *2018 17th ACM/IEEE International Conference on Information Processing in Sensor Networks (IPSN)*. IEEE, 188–199.

[3] F. Ait Aoudia, M. Gautier, and O. Berder. 2018. RLMan: An Energy Manager Based on Reinforcement Learning for Energy Harvesting Wireless Sensor Networks. *IEEE Transactions on Green Communications and Networking* 2, 2 (2018), 408–417. https://doi.org/10.1109/TGCN.2018.2801725

[4] Arm technologies . [n.d.]. https://www.arm.com/technologies/big-little.

[5] Christoph R Birkl, Matthew R Roberts, Euan McTurk, Peter G Bruce, and David A Howey. 2017. Degradation diagnostics for lithium ion cells. *Journal of Power Sources* 341 (2017), 373–386.

[6] BLEHome. 2017. http://www.blehome.com/sensorbug.htm.

[7] Bernhard Buchli, Felix Sutton, Jan Beutel, and Lothar Thiele. 2014. Dynamic power management for long-term energy neutral operation of solar energy harvesting systems. In *Proceedings of the 12th ACM conference on embedded network sensor systems*. 31–45.

[8] Michael Buettner, Ben Greenstein, and David Wetherall. 2011. Dewdrop: An Energy-Aware Runtime for Computational RFID. In *Proceedings of the 8th USENIX Conference on Networked Systems Design and Implementation* (Boston, MA) *(NSDI'11)*. USENIX Association, USA, 197–210.

[9] Bradford Campbell and Prabal Dutta. 2014. An energy-harvesting sensor architecture and toolkit for building monitoring and event detection. In *Proceedings of the 1st ACM Conference on Embedded Systems for Energy-Efficient Buildings*. 100–109.

[10] CISION newswire. 2016. https://www.prnewswire.com/news-releases/worldwide-energy-harvesting-system-market-2020-to-2025---use-of-sensors-in-wearable-electronics-presents-opportunities-301031712.html.

[11] Alexei Colin and Brandon Lucia. 2016. Chain: Tasks and Channels for Reliable Intermittent Programs. In *Proceedings of the 2016 ACM SIGPLAN International Conference on Object-Oriented Programming, Systems, Languages, and Applications* (Amsterdam, Netherlands) *(OOPSLA 2016)*. Association for Computing Machinery, New York, NY, USA, 514–530. https://doi.org/10.1145/2983990.2983995

[12] Alexei Colin, Emily Ruppel, and Brandon Lucia. 2018. A Reconfigurable Energy Storage Architecture for Energy-Harvesting Devices. *SIGPLAN Not.* 53, 2 (March 2018), 767–781. https://doi.org/10.1145/3296957.3173210

[13] Samuel DeBruin, Bradford Campbell, and Prabal Dutta. 2013. Monjolo: An Energy-Harvesting Energy Meter Architecture. In *Proceedings of the 11th ACM Conference on Embedded Networked Sensor Systems* (Roma, Italy) *(SenSys '13)*. Association for Computing Machinery, New York, NY, USA, Article 18, 14 pages. https://doi.org/10.1145/2517351.2517363

[14] e-peas. [n.d.]. https://e-peas.com/product/aem10941/, year = 2018.

[15] Francesco Fraternali, Bharathan Balaji, and Rajesh Gupta. 2018. Scaling Configuration of Energy Harvesting Sensors with Reinforcement Learning. In *Proceedings of the 6th International Workshop on Energy Harvesting amp; Energy-Neutral Sensing Systems* (Shenzhen, China) *(ENSsys '18)*. Association for Computing Machinery, New York, NY, USA, 7–13. https://doi.org/10.1145/3279755.3279760

[16] Raffaele Guida, Neil Dave, Francesco Restuccia, Emrecan Demirors, and Tommaso Melodia. 2019. U-Verse: A Miniaturized Platform for End-to-End Closed-Loop Implantable Internet of Medical Things Systems. In *Proceedings of the 17th Conference on Embedded Networked Sensor Systems* (New York, New York) *(SenSys '19)*. Association for Computing Machinery, New York, NY, USA, 311–323. https://doi.org/10.1145/3356250.3360026

[17] Josiah Hester, Lanny Sitanayah, and Jacob Sorber. 2015. Tragedy of the Coulombs: Federating Energy Storage for Tiny, Intermittently-Powered Sensors. In *Proceedings of the 13th ACM Conference on Embedded Networked Sensor Systems* (Seoul, South Korea) *(SenSys '15)*. Association for Computing Machinery, New York, NY, USA, 5–16. https://doi.org/10.1145/2809695.2809707

[18] Josiah Hester, Lanny Sitanayah, and Jacob Sorber. 2015. Tragedy of the coulombs: Federating energy storage for tiny, intermittently-powered sensors. In *Proceedings of the 13th ACM Conference on Embedded Networked Sensor Systems*. 5–16.

[19] Josiah Hester and Jacob Sorber. 2017. Flicker: Rapid prototyping for the batteryless internet-of-things. In *Proceedings of the 15th ACM Conference on Embedded Network Sensor Systems*. 1–13.

[20] Josiah Hester and Jacob Sorber. 2017. The Future of Sensing is Batteryless, Intermittent, and Awesome. In *Proceedings of the 15th ACM Conference on Embedded Network Sensor Systems* (Delft, Netherlands) *(SenSys '17)*. Association for Computing Machinery, New York, NY, USA, Article 21, 6 pages. https://doi.org/10.1145/3131672.3131699

[21] R. C. Hsu, C. Liu, and H. Wang. 2014. A Reinforcement Learning-Based ToD Provisioning Dynamic Power Management for Sustainable Operation of Energy Harvesting Wireless Sensor Node. *IEEE Transactions on Emerging Topics in Computing* 2, 2 (2014), 181–191. https://doi.org/10.1109/TETC.2014.2316518

[22] Roy Chaoming Hsu, Cheng-Ting Liu, and Wei-Ming Lee. 2009. Reinforcement learning-based dynamic power management for energy harvesting wireless sensor network. In *International Conference on Industrial, Engineering and Other Applications of Applied Intelligent Systems*. Springer, 399–408.

[23] Roy Chaoming Hsu, Cheng-Ting Liu, and Hao-Li Wang. 2014. A reinforcement learning-based ToD provisioning dynamic power management for sustainable operation of energy harvesting wireless sensor node. *IEEE Transactions on Emerging Topics in Computing* 2, 2 (2014), 181–191.

[24] Neal Jackson, Joshua Adkins, and Prabal Dutta. 2019. Capacity over capacitance for reliable energy harvesting sensors. In *Proceedings of the 18th International Conference on Information Processing in Sensor Networks*. 193–204.

[25] Daniel Hsing Po Kang, Mengjun Chen, and Oladele A Ogunseitan. 2013. Potential environmental and human health impacts of rechargeable lithium batteries in electronic waste. *Environmental science & technology* 47, 10 (2013), 5495–5503.

[26] Aman Kansal, Jason Hsu, Sadaf Zahedi, and Mani B. Srivastava. 2007. Power Management in Energy Harvesting Sensor Networks. *ACM Trans. Embed. Comput. Syst.* 6, 4 (Sept. 2007), 32–es. https://doi.org/10.1145/1274858.1274870

[27] KickSat. 2011. https://kicksat.github.io/.

[28] Guohao Lan, Dong Ma, Weitao Xu, Mahbub Hassan, and Wen Hu. 2017. CapSense: Capacitor-Based Activity Sensing for Kinetic Energy Harvesting Powered Wearable Devices. In *Proceedings of the 14th EAI International Conference on Mobile and Ubiquitous Systems: Computing, Networking and Services* (Melbourne, VIC, Australia) *(MobiQuitous 2017)*. Association for Computing Machinery, New York, NY, USA, 106–115. https://doi.org/10.1145/3144457.3144459

[29] Dominique Larcher and Jean-Marie Tarascon. 2015. Towards greener and more sustainable batteries for electrical energy storage. *Nature chemistry* 7, 1 (2015), 19–29.

[30] Brandon Lucia, Vignesh Balaji, Alexei Colin, Kiwan Maeng, and Emily Ruppel. 2017. Intermittent computing: Challenges and opportunities. In *2nd Summit on Advances in Programming Languages (SNAPL 2017)*. Schloss Dagstuhl-Leibniz-Zentrum fuer Informatik.

[31] Yunfei Ma, Zhihong Luo, Christoph Steiger, Giovanni Traverso, and Fadel Adib. 2018. Enabling deep-tissue networking for miniature medical devices. In *Proceedings of the 2018 Conference of the ACM Special Interest Group on Data Communication*. 417–431.

[32] Gang Ning and Branko N Popov. 2004. Cycle life modeling of lithium-ion batteries. *Journal of The Electrochemical Society* 151, 10 (2004), A1584.

[33] Nordic Semiconductor. 2018. Nordic Thingy:52 . https://www.nordicsemi.com/Software-and-tools/Prototyping-platforms/Nordic-Thingy-52#infotabs.

[34] Andrea Ortiz, Hussein Al-Shatri, Xiang Li, Tobias Weber, and Anja Klein. 2017. Reinforcement learning for energy harvesting decode-and-forward two-hop communications. *IEEE Transactions on green communications and networking* 1, 3 (2017), 309–319.

[35] Joshua P Pender, Gaurav Jha, Duck Hyun Youn, Joshua M Ziegler, Ilektra Andoni, Eric J Choi, Adam Heller, Bruce S Dunn, Paul S Weiss, Reginald M Penner, et al. 2020. Electrode degradation in lithium-ion batteries. *ACS nano* 14, 2 (2020), 1243–1295.

[36] Benjamin Ransford, Jacob Sorber, and Kevin Fu. 2011. Mementos: System Support for Long-Running Computation on RFID-Scale Devices. In *Proceedings of the Sixteenth International Conference on Architectural Support for Programming Languages and Operating Systems* (Newport Beach, California, USA) *(ASPLOS XVI)*. Association for Computing Machinery, New York, NY, USA, 159–170. https://doi.org/10.1145/1950365.1950386

[37] Yohann Rioual, Yannick Le Moullec, Johann Laurent, Muhidul Islam Khan, and Jean-Philippe Diguet. 2018. Reward function evaluation in a reinforcement learning approach for energy management. In *2018 16th Biennial Baltic Electronics Conference (BEC)*. IEEE, 1–4.

[38] Nurani Saoda, Md Fazlay Rabbi Masum Billah, and Bradford Campbell. 2021. Designing a General Purpose Development Platform for Energy-harvesting Applications. In *Proceedings of the 19th ACM Conference on Embedded Networked Sensor Systems*. 581–583.

[39] Nurani Saoda and Bradford Campbell. 2019. No Batteries Needed: Providing Physical Context with Energy-Harvesting Beacons. In *Proceedings of the 7th International Workshop on Energy Harvesting amp; Energy-Neutral Sensing Systems* (New York, NY, USA) *(ENSsys'19)*. Association for Computing Machinery, New York, NY, USA, 15–21. https://doi.org/10.1145/3362053.3363489

[40] Alexander Sarris. 2020. *LPCSB: A Device to Distinguish Between Natural and Artificial Light(Afrikaans Text)*. Master's thesis. AAI0662099.

[41] Shaswot Shresthamali, Masaaki Kondo, and Hiroshi Nakamura. 2017. Adaptive power management in solar energy harvesting sensor node using reinforcement learning. *ACM Transactions on Embedded Computing Systems (TECS)* 16, 5s (2017), 1–21.

[42] Rishi Shukla, Neev Kiran, Rui Wang, Jeremy Gummeson, and Sunghoon Ivan Lee. 2019. SkinnyPower: enabling batteryless wearable sensors via intra-body

power transfer. In *Proceedings of the 17th Conference on Embedded Networked Sensor Systems*. 68–82.

[43] STMicroelectronics. [n.d.]. https://www.st.com/resource/en/datasheet/stm32wb10cc.pdf.

[44] Richard S. Sutton and Andrew G. Barto. 2018. *Reinforcement Learning: An Introduction*. A Bradford Book, Cambridge, MA, USA.

[45] Texas Instruments. [n.d.]. https://www.ti.com/product/CC2640#design-development.

[46] Hoang Truong, Shuo Zhang, Ufuk Muncuk, Phuc Nguyen, Nam Bui, Anh Nguyen, Qin Lv, Kaushik Chowdhury, Thang Dinh, and Tam Vu. 2018. Capband: Battery-free successive capacitance sensing wristband for hand gesture recognition. In *Proceedings of the 16th ACM Conference on Embedded Networked Sensor Systems*. 54–67.

[47] Feixiang Wu, Joachim Maier, and Yan Yu. 2020. Guidelines and trends for next-generation rechargeable lithium and lithium-ion batteries. *Chemical Society Reviews* 49, 5 (2020), 1569–1614.

[48] L. Yerva, B. Campbell, A. Bansal, T. Schmid, and P. Dutta. 2012. Grafting energy-harvesting leaves onto the sensornet tree. In *2012 ACM/IEEE 11th International Conference on Information Processing in Sensor Networks (IPSN)*. 197–207. https://doi.org/10.1109/IPSN.2012.6920957

[49] Ting Zhu, Ziguo Zhong, Yu Gu, Tian He, and Zhi-Li Zhang. 2009. Leakage-Aware Energy Synchronization for Wireless Sensor Networks. In *Proceedings of the 7th International Conference on Mobile Systems, Applications, and Services* (Kraków, Poland) *(MobiSys '09)*. Association for Computing Machinery, New York, NY, USA, 319–332. https://doi.org/10.1145/1555816.1555849